CHAPTER 4

POLYSACCHARIDE FROM *LENTINUS FUSIPES*

A part of this chapter has been published in the following article:

1. D. K. Manna, Ashis K. Nandi, M. Pattanayak, P. Maity, A. K. Mandal, N. Gupta and S. S. Islam. Carbohydrate Polymer. 157, 1657-1565, 2017.

4.1. Introduction and review of earlier works

The edible mushroom, *Lentinus fusipes*, belongs to the genus *Lentinus*, family *Polyporaceae*, mostly grows below bamboo clumps during rainy season. Therefore, it is locally known as baunsa chattu [19]. The most promising polysaccharide isolated from Shiitake mushroom, *Lentinus edodes* is Lentinan [82-84] which exhibits antitumor and anti-cancer property. The goal of this study is to determine the structural characteristics and immunostimulating activities of the polysaccharides of the fruiting body of *Lentinus fusipes*. Two water soluble polysaccharides (PS-I & PS-II) have been isolated from the aqueous extract of this mushroom. The detailed structural characterization and biological properties of PS-II were carried out and include in this chapter of the thesis.

4.2. Present work

4.2.1. Isolation and purification of polysaccharides from *Lentinus fusipes*

The crude polysaccharide (2.1 g) was isolated from the mushroom by boiling the dried fruit bodies (50 g) with distilled water at 100 °C for 10 h, followed by precipitation in EtOH (5:1), dialysis, centrifugation and freeze drying. A portion of the crude polysaccharide was purified by fractionation through Sepharose 6B GPC column [203]. The crude polysaccharide (25 mg) yielded two homogeneous fractions, PS-I (test tube 30–42) and PS-II (test tube 54–68) (**Figure 4.1**). These are collected and freeze-dried to yield pure PS-I (9 mg) and PS-II (11 mg). The same procedure was repeated for 10 times to yield 81 mg pure of PS-I and 103 mg of PS-II. The second fraction, PS-II produced a single symmetrical peak on further purification by GPC indicating it was homogeneous. The detailed structural investigation and biological activities of PS-II were investigated and presented in this chapter.

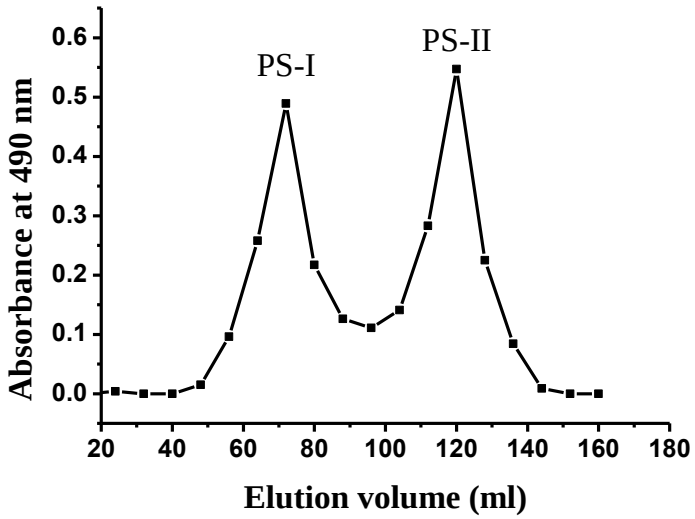

Figure 4.1. Chromatogram of crude polysaccharide isolated from an edible mushroom *L. fusipes* using Sepharose 6B column.

4.2.2. Optical rotation and molecular weight of PS-II

The average molecular weight of PS-II was calculated as ~ 60 kDa from the calibration curve prepared using standard dextrans (**Figure 4.2**). The PS-II showed specific rotation $[\alpha]_D^{31}$ -8.6 (*c* 0.15, water).

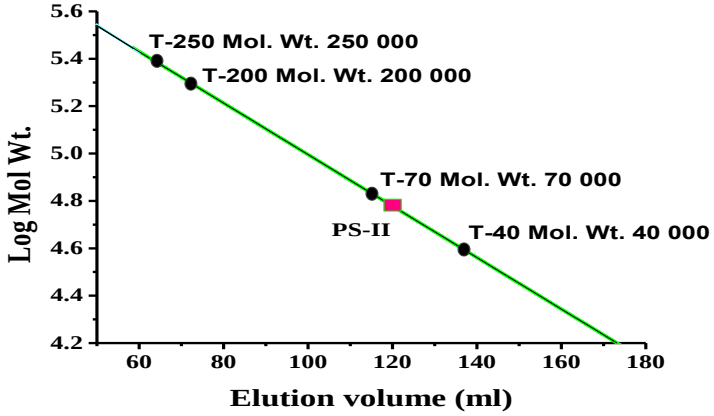

Figure 4.2. Determination of molecular weight PS-II isolated from mushroom *L. fusipes.*

4.2.3. Structural analysis of PS-II

4.2.3.1. Chemical analysis of PS-II

GLC analysis of the alditol acetates derived from PS-II by acid hydrolysis showed the presence of galactose and glucose in a molar ratio of approximately 1:1. The absolute configuration of all monomeric sugar units had the D configuration that was determined by the method of Gerwig et al., 1978 [206]. The linkage pattern and ratio of the monomeric units present in PS-II was determined by methylation analysis using the method of Ciucanu and Kerek (1984) [207], followed by hydrolysis with HCOOH and preparation of alditol acetates. The GLC-MS analysis of the alditol acetates of methylated and hydrolysed products showed the presence of 1,5-di-O-acetyl-2,3,4,6-tetra-O-methyl-D-glucitol, 1,5,6-tri-O-acetyl-2,3,4-tri-O-methyl-D-glucitol, 1,3,5-tri-O-acetyl-2,4,6-tri-O-methyl-D-galactol and 1,3,5,6-tetra-O-acetyl-2,4-di-O-methyl-D-glucitol in a molar ratio of nearly 1:1:3:1 respectively. The GLC-MS chromatogram and the methylation analysis products are shown in the following **Figure 4.3 & 4.4.** The mass fragments result of the methylated products is presented in **Table 4.1.** These results indicated the presence of terminal glucopyranosyl, (1→6), (1→3, 6)-linked and (1→6)-linked galactopyranosyl residues.

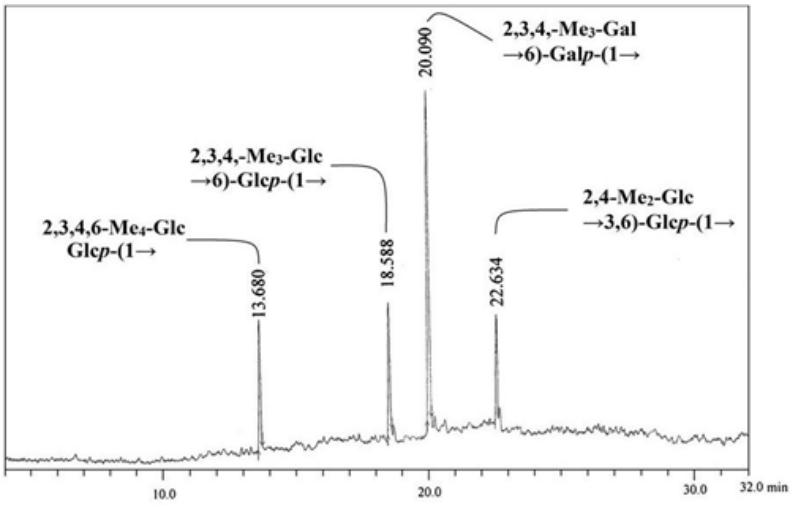

Figure 4.3: GLC-MS analysis of alditol acetates of methylated PS-II.

Table 4.1. GLC-MS analysis of methylated PS-II isolated from mushroom *L. fusipes.*

Methylated sugars	Molar ratio	Linkage type	Major Mass Fragments (m/z)
2,3,4,6-Me_4-Glc	1	Glc*p*-(1→	41,43,59,71,87,101,117,129,145, 161,173,192,205,219
2,3,4,-Me_3-Gal	3	→6)-Gal*p*-(1→	41,43,58,71,87,101,117,129,143, 161,173,189,203,221,233
2,3,4,-Me_3-Glc	1	→6)-Glc*p*-(1→	41,43,58,71,87,101,117,129,143, 161,173,189,203,221,233
2,4-Me_2-Glc	1	→3,6)-Glc*p*-(1→	40,43,58,74,87,99,101,117,129,1 43,159173,189,207,217,233,245,

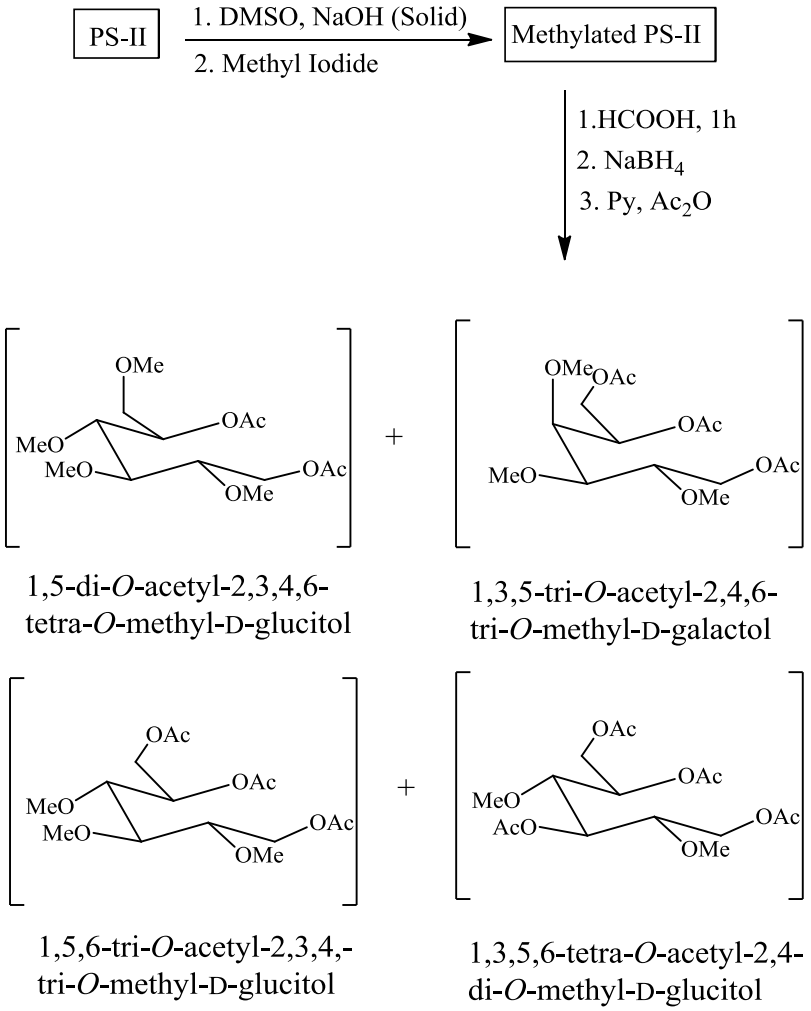

Figure 4.4. Schematic presentation of methylation experiment of PS-II.

According to these results there are the possibility of a (1→6)-linked backbone. The GLC analysis of the alditol acetates of the periodate-oxidised [241], $NaBH_4$ reduced PS-II showed the presence of only D-glucose and GLC-MS analysis of periodate-oxidised, reduced, methylated [242] PS-II showed the presence of 1,3,5,6-tetra-*O*-acetyl-2,4-di-*O*-methyl-D-glucitol which are presented in **Table 4.2** and **Figure 4.5**. These results indicated that during oxidation of the PS-II consisting (1→6)-D-Gal*p*, (1→6)-D-Glc*p* and terminal D-Glc*p* residues were consumed keeping (1→3, 6)-D-Glc*p* residue intact.

Table 4.2. GLC-MS analysis of periodate-oxidised, reduced, methylated PS-II.

Methylated sugars	Linkage type	Major Mass Fragments (m/z)
2,4-Me_2-Glc	→3,6)-β-D-Glc*p*-(1→	40,43,58,74,87,101,117,129,143, 159,173,189,200,235,245

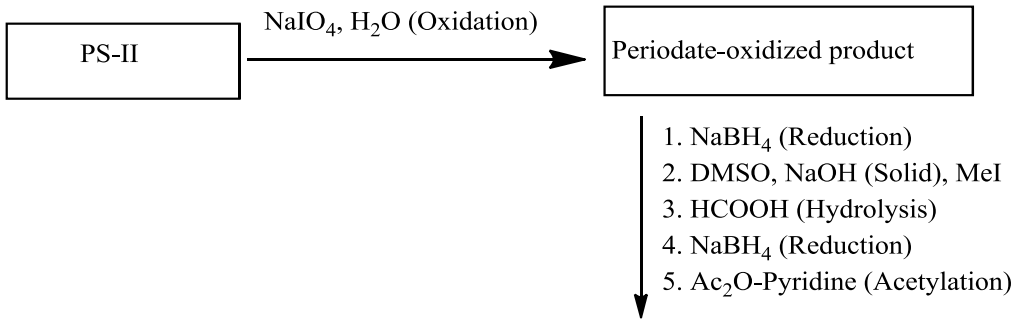

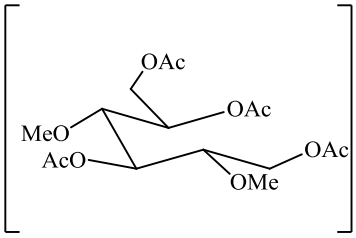

1,3,5,6-tetra-*O*-acetyl-2,4-di-*O*-methyl-D-glucitol

Figure 4.5. Schematic presentation of periodate oxidation reactions of PS-II.

4.2.3.2. Spectroscopic analysis of PS-II

❖ FT-IR analysis

The FT-IR spectra (**Figure 4.6,** as shown below**)** of PS-II showed a strong and broad band around 3414 cm^{-1} is the characteristic of O-H stretching frequency [244]. The peak at 2925 is assigned to aliphatic C-H stretching [245]. The absorption peaks at 1630, 1399, 1158 and 1077 cm^{-1} are assigned to bound water, bending vibration of C-OH [246], C-O stretching of ether [247] as well as C-C stretching and anti-symmetric stretching band of C-O-C groups of polysaccharides [246], respectively. A characteristic absorption at 880 was also observed, indicating the presence of β-D-glucopyranose [248-249] and the band at 809 is characteristic absorption of α-D-galactopyranose [250] in PS-II.

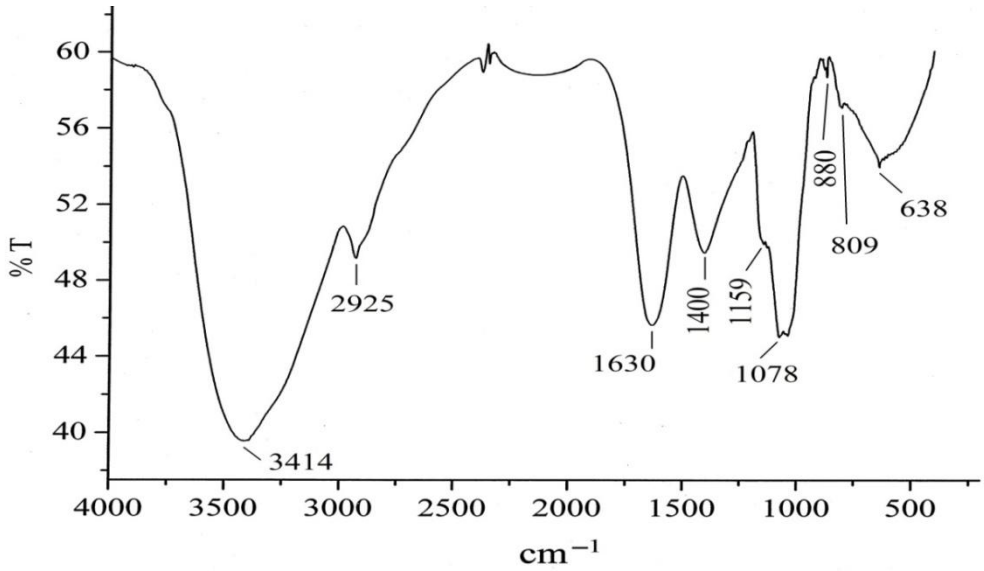

Figure 4.6. FT-IR spectrum of PS-II isolated from an edible mushroom *L. fusipes.*

❖ NMR and structural analysis of PS-II

The ^{1}H NMR (700 MHz) spectrum (**Figure 4.7**) at 30 ºC showed six signals in the anomeric region at δ 5.08, 5.01, 5.00, 4.54, 4.53 and 4.52. They were designated as **A** to **F** residues according to their decreasing proton chemical shift values. In the ^{13}C (175 MHz) spectrum (**Figure 4.8**) at 30 ºC five anomeric signals appeared at δ 103.0, 102.9,102.8, 101.5, and δ 98. The other carbon signals came in the region δ 84.5–60.6. The anomeric carbon chemical shift values of residues **A** to **F** were correlated to the anomeric proton signals of residues from the HSQC spectrum

(**Figure 4.9a**). The anomeric carbon signal at δ 103.0 correlated to anomeric proton signal of **D (**δ 4.54**)**, δ 102.9 correlated to the signals **E (**δ 4.53**)**, the signal at δ 102.8 correlated to **F (**δ 4.52**),** the signal at δ 101.5 correlated to **A (**δ 5.09**)** and 98.0 correlated to both **B (**δ 5.01**)** and **C (**δ 5.00**)** residues respectively.

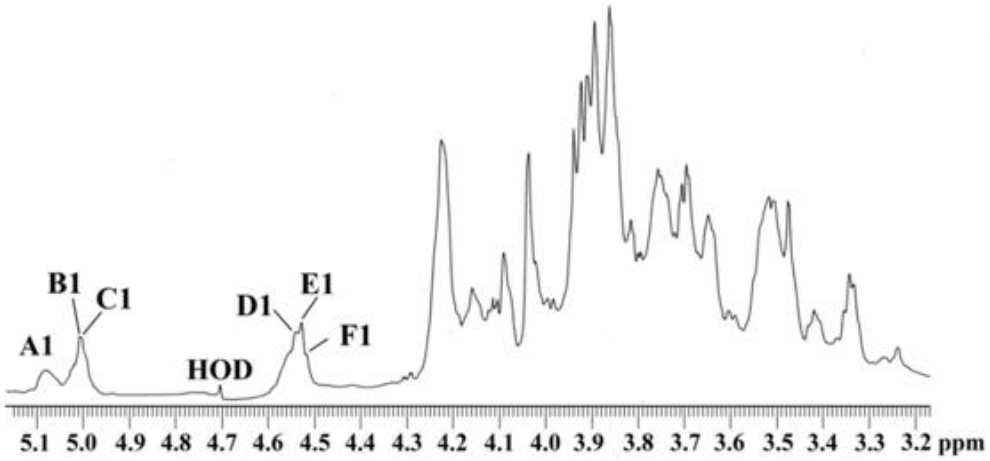

Figure 4.7. ^{1}H NMR spectrum (700MHz, D_2O, 30 ºC) of PS-II

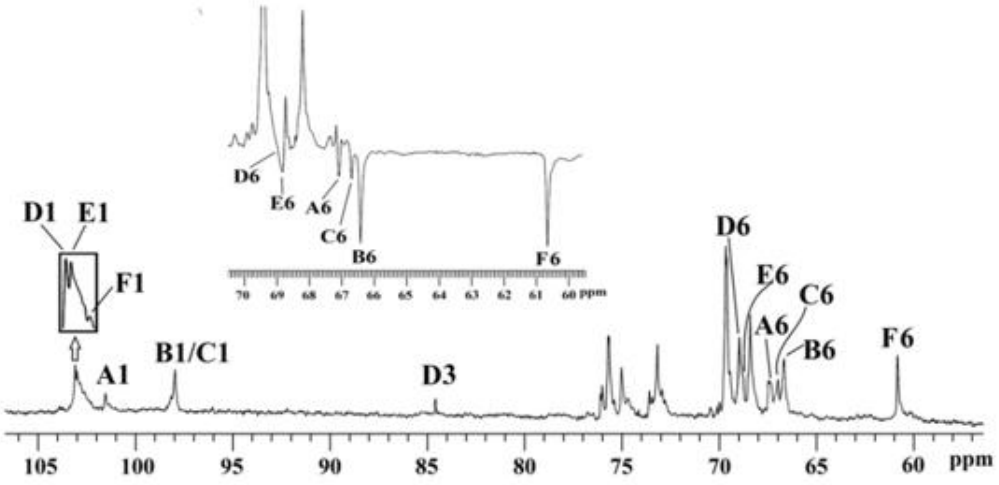

Figure 4.8. ^{13}C NMR spectrum (175MHz, D_2O, 30 ºC) and part of DEPT-135 spectrum (D_2O, 30 ºC) (inset) of PS-II.

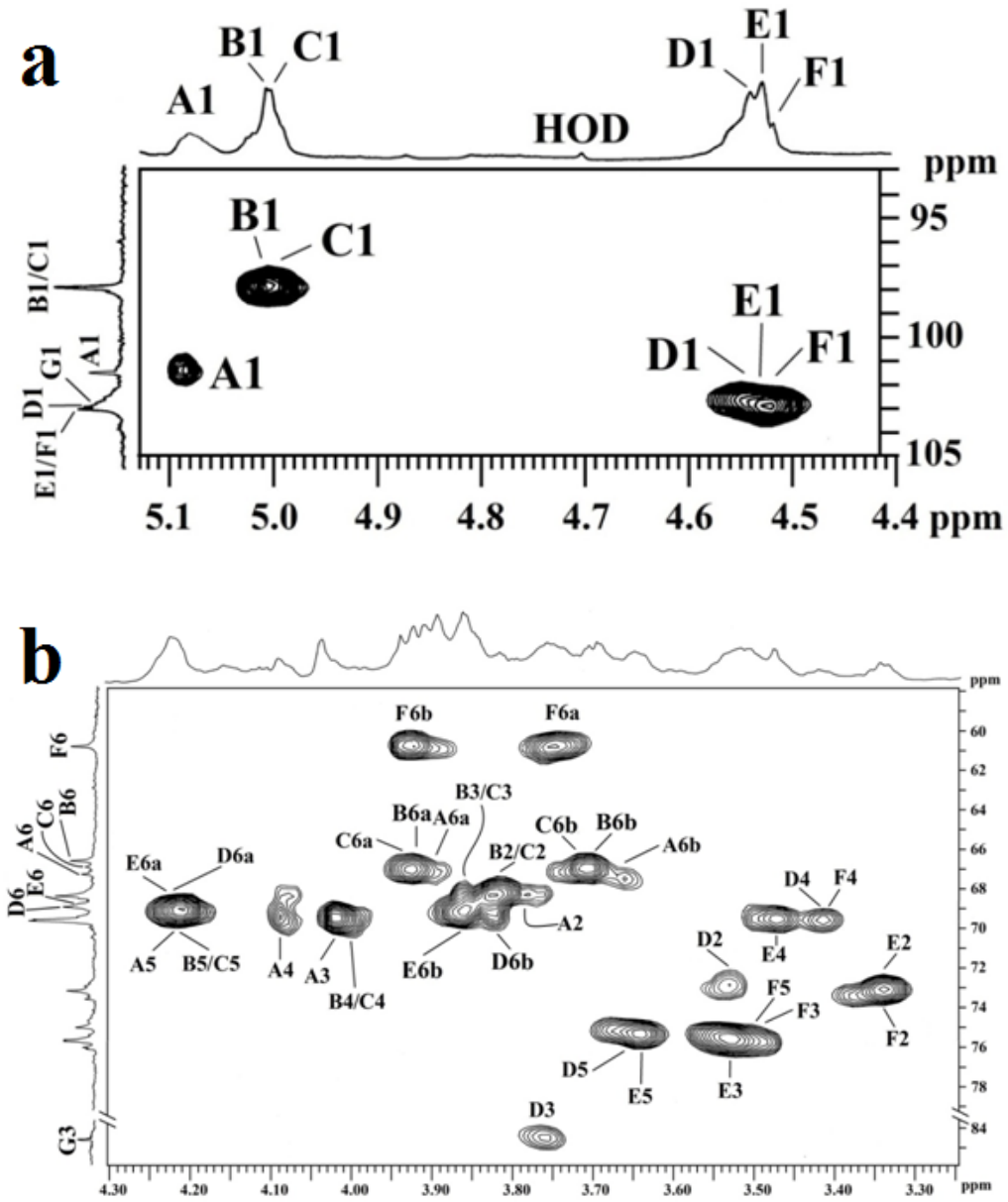

Figure 4.9. The HSQC spectrum of (a) anomeric part and (b) other than anomeric part of PS-II.

All the ^{1}H and ^{13}C signals (shown in **Table 4.3**) were assigned using DQF-COSY, TOCSY and HSQC (**Figure 4.9a & b**) experiments. The proton coupling constants were measured from DQF-COSY experiment.

Table 4.3. The ^{1}H NMR[a] and ^{13}C NMR[b] chemical shifts of PS-II.

Glucosyl residue	H-1/ C-1	H-2/ C-2	H-3/ C-3	H-4/ C-4	H-5/ C-5	H-6a,H-6b/ C-6
→6)-α-D-Gal*p*-(1→	5.08	3.79	4.02	4.09	4.22	3.90[c],3.66[d]
A	101.5	68.4	69.7	69.2	69.5	67.2
→6)-α-D-Gal*p*-(1→	5.01	3.82	3.86	4.00	4.21	3.92[d],3.70[c]
B	98.0	68.2	69.4	69.3	69.4	66.4
→6)-α-D-Gal*p*-(1→	5.00	3.82	3.86	4.00	4.21	3.94[d],3.72[c]
C	98.0	68.2	69.4	71.6	69.4	66.7
→3,6)-β-D-Glc*p*-(1→	4.54	3.52	3.76	3.42	3.66	4.22[c], 3.82[d]
D	103.0	72.9	84.5	69.6	75.5	68.8
→6)-β-D-Glc*p*-(1→	4.53	3.34	3.53	3.47	3.64	4.23[c], 3.86[d]
E	102.9	73.2	75.9	69.5	75.3	68.7
β-D-Glc*p*-(1→	4.52	3.34	3.49	3.41	3.50	3.92[c], 3.75[d]
F	102.8	73.2	75.8	69.6	76.0	60.6

[a]The values of chemical shifts were recorded keeping HOD signal fixed at δ 4.70 at 30 ºC.

[b] The values of chemical shifts were recorded with reference to acetone as internal standard and fixed at δ 31.05 at 30 ºC.

[c,d] Interchangeable.

The residues **A**, **B** and **C** were assigned to Gal*p* configuration from large $J_{H\text{-}2,H\text{-}3}$ coupling constant (~8 Hz) and relatively small $J_{H\text{-}3,H\text{-}4}$ coupling constant (~3 Hz). The α-configuration of all **A**-**C** residues were assigned from $J_{H\text{-}1,H\text{-}2}$ coupling constant (~3 Hz) and $J_{C\text{-}1,H\text{-}1}$ (~170 Hz) for anomeric proton chemical shift (δ 5.08 for **A**, δ 5. 01 for **B** and δ 5. 00 for **C**) and carbon chemical shift (δ 101.5 for **A**, 98.0 for **B** and **C**). The downfield appearance of the carbon chemical shifts of C-6 (δ 67.2, 66.4 and 66.7 respectively) for **A**, **B** and **C** with respect to the standard values of methyl glycosides indicated that these residues were linked at C-6. The linkages at C-6 of the residues **A**-**C** were further confirmed from DEPT-135 spectrum, as shown below Figure 4.8. Thus, **A**-**C** residues were confirmed as (1→6)-α-D-Gal*p*.

Residues **D**-**F** were established as β-configuration from coupling constant values $J_{H\text{-}1,H\text{-}2}$ (~8.0 Hz), $J_{C\text{-}1,H\text{-}1}$ (~160 Hz) and the large $J_{H\text{-}2,H\text{-}3}$, $J_{H\text{-}3,H\text{-}4}$ coupling

constant values (~10.0 Hz) of **D-F** confirmed their D-Glc*p* configuration. All chemical shift values of residue **F** were found nearly close to the standard values of methyl glycoside of β-D-glucose, evidently indicated that the residue **F** was terminal β-D-glucose. The downfield shifts of C-3 (δ 84.5) and C-6 (δ 68.8) of the residue **D** with respect to the standard values of methyl glycoside indicated that residue **D** was linked at C-3 and C-6. Again, the downfield shift of C-6 (δ 68.7) of **E** residue indicated that it was linked at C-6. The linkages at C-6 of the residues, **D-E** were further confirmed from DEPT-135 spectrum (Figure 4.8, inset). Therefore, all the residues were confirmed as (1→3,6)-β-D-Glc*p* (**D**), (1→6)-β- D-Glc*p* (**E**) and terminal β-D-glc*p* (**F**) respectively.

The sequence of glycosyl residues (**A** to **F**) was determined from ROESY (**Figure 4.10, Table 4.4,**) experiment. In ROESY experiment, the inter-residual contacts **A**H-1/**D**H-6a, 6b; **B**H-1/**C**H-6a, 6b; **C**H-1/**A**H-6a, 6b; **D**H-1/**E**-H6a, 6b; **E**H-1/**B**H-6a, 6b and **F**H-1/**D**H-3 along with other intra-residual contacts were also observed. The above ROESY connectivities established the following sequences: **A** (1→6) **D**; **B** (1→6) **C**; **C** (1→6) **A**; **D** (1→6) **E**; **E** (1→6) **B** and **F** (1→3) **D**.

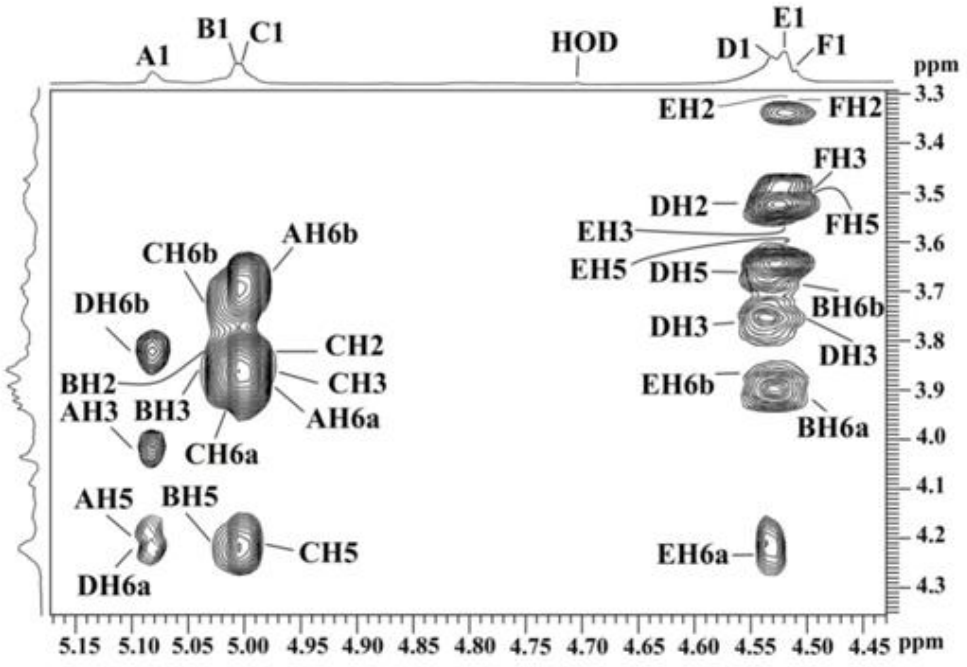

Figure 4.10. Part of ROESY spectrum of PS-II isolated from the mushroom *L. fusipes*. The ROESY mixing time was 300 ms.

Table 4.4. ROESY data for the polysaccharide isolated from the mushroom *L. fusipes*.

Glycosyl residue	Anomeric proton δ	ROE contact proton		
		Δ	residue	Atom
→6)-α-D-Gal*p*-(1→ **A**	5.08	4.22	**D**	H-6a
		3.82	**D**	H-6b
		4.02	**A**	H-3
		4.22	**A**	H-5
→6)-α-D-Gal*p*-(1→ **B**	5.01	3.92	**C**	H-6a
		3.70	**C**	H-6b
		3.82	**B**	H-2
		3.86	**B**	H-3
		4.21	**B**	H-5
→6)-α-D-Gal*p*-(1→ **C**	5.00	3.89	**A**	H-6a
		3.66	**A**	H-6b
		3.82	**C**	H-2
		3.86	**C**	H-3
		4.21	**C**	H-5
→3,6)-β-D-Glc*p*-(1→ **D**	4.54	4.22	**E**	H-6a
		3.82	**E**	H-6b
		3.52	**D**	H-2
		3.76	**D**	H-3
		3.66	**D**	H-5
→6)-β-D-Glc*p*-(1→ **E**	4.53	3.92	**B**	H-6a
		3.70	**B**	H-6b
		3.34	**E**	H-2
		3.53	**E**	H-3
		3.64	**E**	H-5
β-D-Glc*p*-(1→ **F**	4.52	3.76	**D**	H-3
		3.34	**F**	H-2
		3.49	**F**	H-3
		3.50	**F**	H-5

Finally, the ROESY connectivities were confirmed from HMBC spectrum (shown below **Figure 4.11, Table 4.5**). In this spectrum the inter-residual cross-peaks between **A**H-1/**D**C-6, **A**C-1/**D**H-6a, 6b; **B**H-1/**C**C-6, **B**C-1/**C**H-6a, 6b; **C**H-1/**A**C-6, **C**C-1/**A**H-6a; **D**H-1/**E**C-6, **D**C-1/**E**H-6a, 6b; **E**H-1/**B**C-6, **E**C-1/**B**H-6a, 6b and **F**H-1/**D**C-3, **F**C-1/**D**H-**3** along with some intra-residual peaks were also observed.

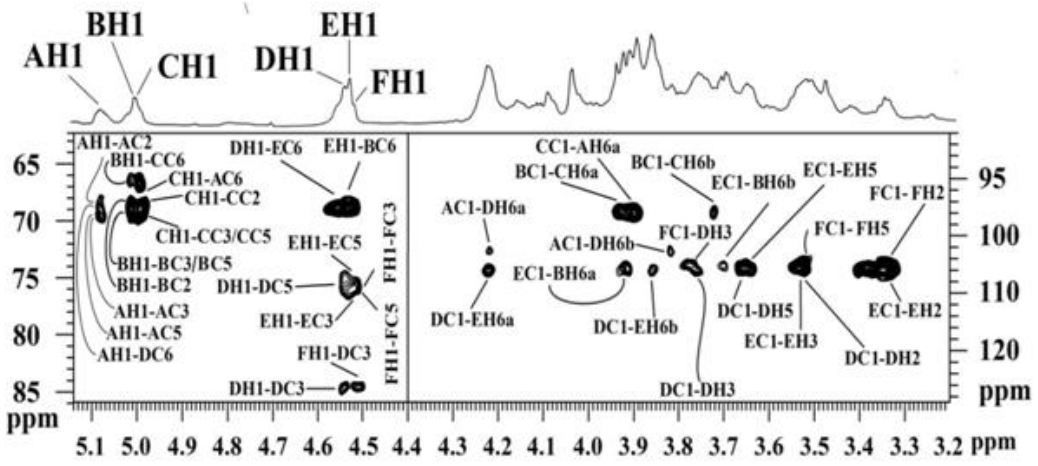

Figure 4.11. Part of the HMBC spectrum of PS-II isolated from the mushroom *L. fusipes.*

Table 4.5. The significant $^{3}J_{H,C}$ connectivities observed in an HMBC spectrum for the anomeric protons/carbons of the sugar residues of PS-II.

Residue	Sugar linkage	H-1/C-1 δ_H / δ_C	Observed connectivities		
			δ_H / δ_C	Residue	Atom
A	→6)-α-D-Gal*p*-(1→	5.08 101.5	68.8	**D**	C-6
			68.2	**A**	C-2
			69.7	**A**	C-3
			69.5	**A**	C-5
			4.22	**D**	H-6a
			3.82	**D**	H-6a
B	→6)-α-D-Gal*p*-(1→	5.01 98.0	66.7	**C**	C-6
			68.2	**B**	C-2
			69.4	**B**	C-3/C-5
			3.94	**C**	H-6a
			3.72	**C**	H-6b
C	→6)-α-D-Gal*p*-(1→	5.00 98.0	67.2	**A**	C-6
			68.2	**C**	C-2
			69.4	**C**	H-3/C-5
			3.90	**A**	H-6a
D	→3,6)-β-D-Glc*p*-(1→	4.54 103.0	68.7	**E**	C-6
			84.5	**D**	C-3
			75.5	**D**	C-5
			4.23	**E**	H-6a
			3.86	**E**	H-6b
			3.52	**D**	H-2
			3.76	**D**	H-3
			3.66	**D**	H-5
E	→6)-β-D-Glc*p*-(1→	4.53 102.9	66.4	**B**	C-6
			75.9	**E**	C-3
			75.3	**E**	C-5
			3.92	**B**	H-6a
			3.70	**B**	H-6b
			3.34	**E**	H-2
			3.53	**E**	H-3
			3.64	**E**	H-5
F	β-D-Glc*p*-(1→	4.52 102.8	84.5	**D**	C-3
			75.8	**F**	C-3
			76.0	**F**	C-5
			3.76	**D**	H-3
			3.34	**F**	H-2
			3.50	**F**	H-5

Hence, based on all these chemical and spectroscopic experimental results the structure of the repeating motif of PS-II was proposed as:

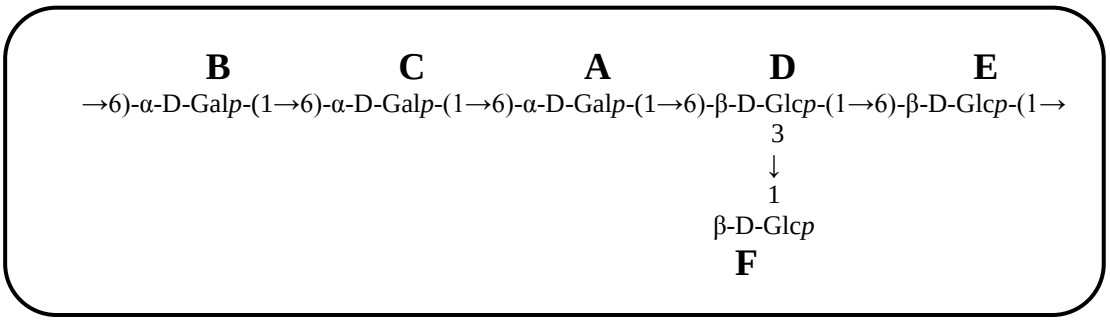

On the other hand, Smith degraded material (SDM) of PS-II was prepared to confirm the linkages of the heteroglycan. The ^{13}C NMR (125 Hz) spectrum (shown below **Figure 4.12, Table 4.6**) of SDM at 30 ^{o}C showed only one anomeric carbon signal at δ 102.1 which corresponded to β-D-Glc*p* (**H**). The carbon signals C-1, C-2, and C-3 of the glycerol moiety (**Gro, I**) were assigned at δ 66.5, 72.0 and 62.5, respectively. Due to the oxidation followed by degradation, all residues (**A**-**F**) except **D** were consumed and **D** was converted to β-D-Glc*p* (**G**). The glycerol moiety (Gro) was generated after Smith degradation from the residue (1→6)-β-D-Glc*p* (**E**) which was directly attached to the **D** residue of the parent PS. Hence, Smith degradation had resulted in the formation of a glycerol containing monosaccharide from PS-II and the structure of SDM was established as:

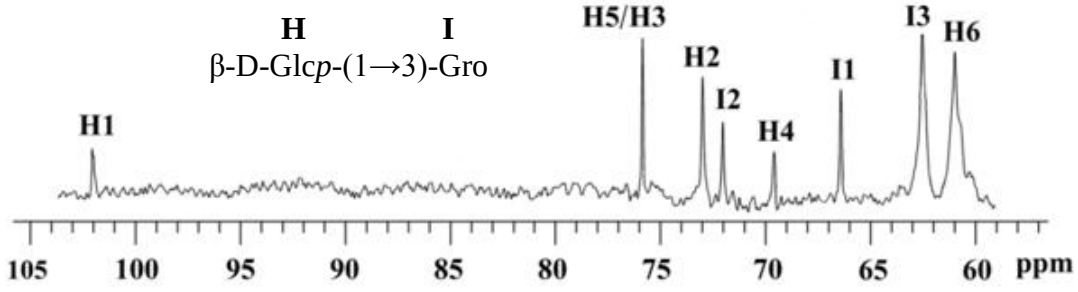

Figure 4.12. ^{13}C NMR spectrum (125MHz, D_2O, 30 ºC) of Smith-degraded glycerol-containing material of PS-II.

Table 4.6. The ^{13}C NMR[n] chemical shifts of Smith-degraded glycerol-containing material of the mushroom *L. fusipes* in D_2O at 30 ºC.

Sugar residue	C-1	C-2	C-3	C-4	C-5	C-6
β-D-Glc*p*-(1→ **H**	102.1	73.0	76.0	69.5	76.0	61.0
Gro-(3→ **I**	66.5	72.0	62.5			

[n] The values of chemical shifts were recorded with reference to acetone as internal standard and fixed at δ 31.05 at 30 ºC.

Therefore, the results of Smith degradation clearly indicated that the repeating unit of the PS-II had a backbone chain consisting of three residues of (1→6)-α-D-Gal*p* and two residues of (1→6)-β-D-Glc*p*, out of which one β-D-Glc*p* residue was branched at *O*-3 position with a terminal β-D-Glc*p*.

4.2.4. Biological studies of PS-II

4.2.4.1. Cell viability study by MTT assay

The cytotoxic effect of the PS-II was studied on human blood lymphocytes at varied concentrations ranging from 20 µg/ml to 320 µg/ml. MTT study suggested that the PS-II exhibited no considerable cytotoxic effect on lymphocytes. Cell proliferative activity was observed significantly ($p<0.05$) up to 160 µg/ml but 320 µg/ml dosage of PS-II showed mild toxicity (**Figure 4.13**). Previous reports showed that polysaccharides extracted from mushroom *Termitomyces heimii* [57] showed cellular toxicity above 200 µg/ml of PS. Whereas, PS extracted from *Entoloma lividoalbum* and bacterium *Klebsiella pneumoniae* PB12 showed cellular toxicity above 100 µg/ml of PS dosage [61,243].

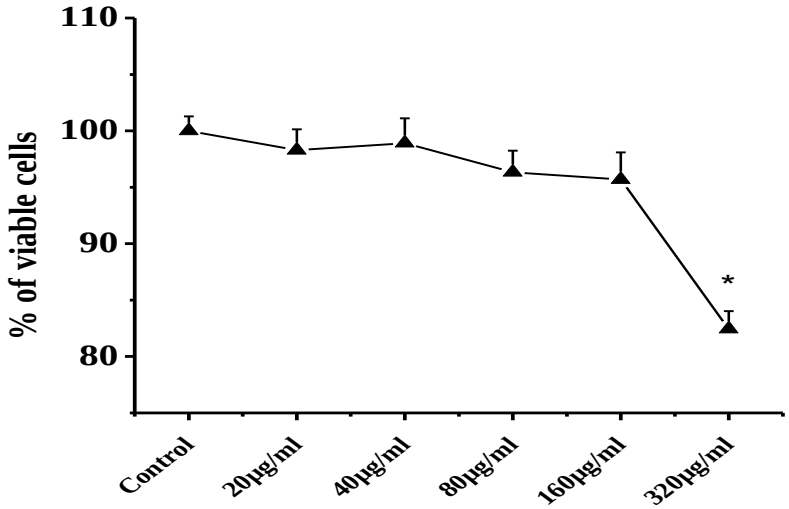

Figure 4.13. MTT assay showing in-vitro cytotoxicity of PS-II on peripheral blood lymphocytes. (n = 4, values are expressed as mean±SEM. * Indicates the significant difference as compared to control group).

4.2.4.2. Determination of reduced glutathione (GSH) and oxidizedglutathione (GSSG) level

An important antioxidant, glutathione, was measured both in its reduced and oxidized forms in the cellular system (**Figure 4.14 & Figure 4.15**). Results showed that the reduced glutathione (GSH) level significantly increased up to 160 µg/ml of PS-II, whereas at concentration 320 µg/ml, it was moderately decreased but slight increase in GSSG level was observed. It was noted that the redox ratio (GSH/GSSG) alteration is fully correlated with variation in PS-II concentrations (Pearson Co-efficient r= 0.951, Pearson correlation $p < 0.05$).

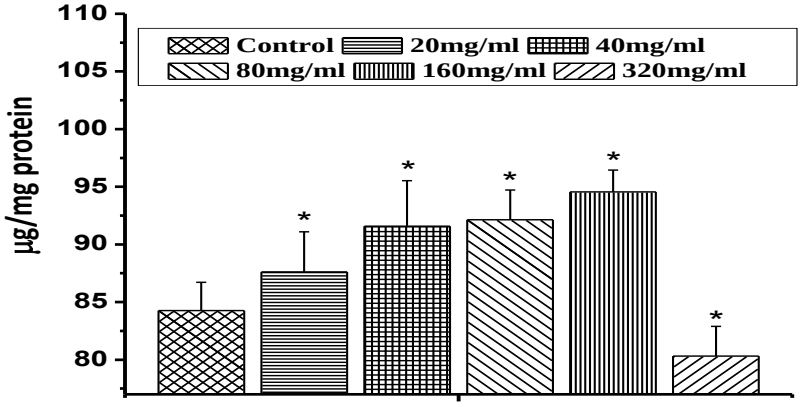

Figure 4.14. Concentration of reduced glutathione (GSH) level in normal human lymphocytes treated with different concentrations of PS-II. (n = 4, values are expressed as mean±SEM. * Indicates the significant difference as compared to control group).

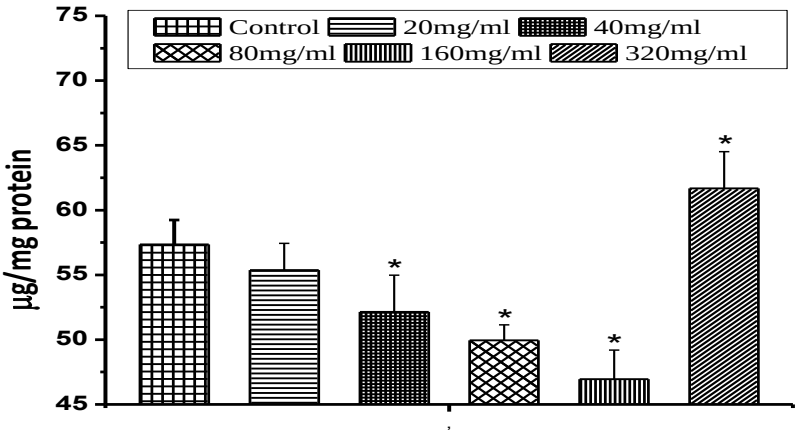

Figure 4.15. Concentration of oxidized glutathione (GSSG) level in normal human lymphocytes treated with different concentrations of PS-II. (n = 4, values are expressed as mean±SEM. * Indicates the significant difference as compared to control group).

4.2.4.3. Determination of lipid peroxidation (MDA)

In order to assess the cellular status in presence of reactive oxygen species (ROS), lipid peroxidation assay was determined and degree of lipid peroxidation can be measured in terms of malondialdehyde (MDA) production. Our result exhibited increase in MDA production in the presence of 320 µg/ml of PS-II (**Figure 4.16**).

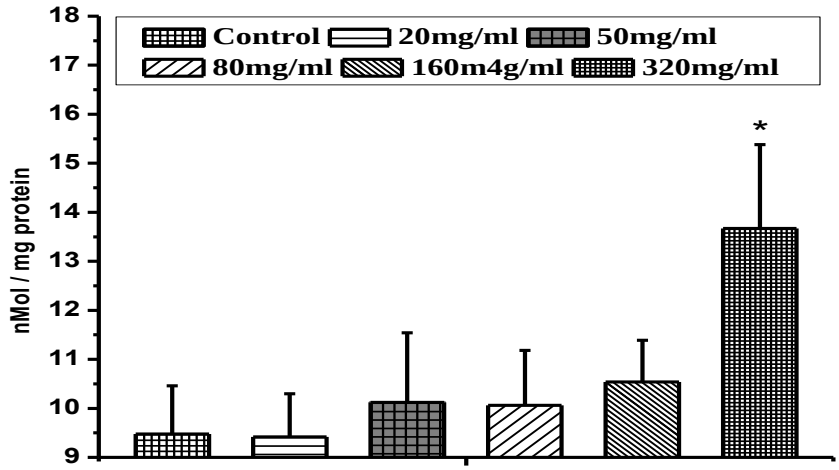

Figure 4.16. Concentration of MDA level of PS-II treated normal human lymphocytes toevaluate lipid peroxidation. (n = 4, values are expressed as mean±SEM. * Indicates the significant difference as compared to control group).

4.2.4.4. Protective role against nicotine toxicity

In order to establish the protective role against nicotine toxicity by PS-II, lymphocytes were impregnated with nicotine (10 mM) alone and PS-II (160 µg/ml) + nicotine (10 mM) for 24 h in culture media. Flow cytometry study revealed the protective role of PS-II against nicotine toxicity. It was noted that there is a decrease in fluorescence intensity of propidium iodide (PI) in the nicotine stimulated cells when treated with PS-II (**Figure 4.17a & 4.17b**). This decrease in fluorescence intensity was possibly due to ROS scavenging property of PS-II.

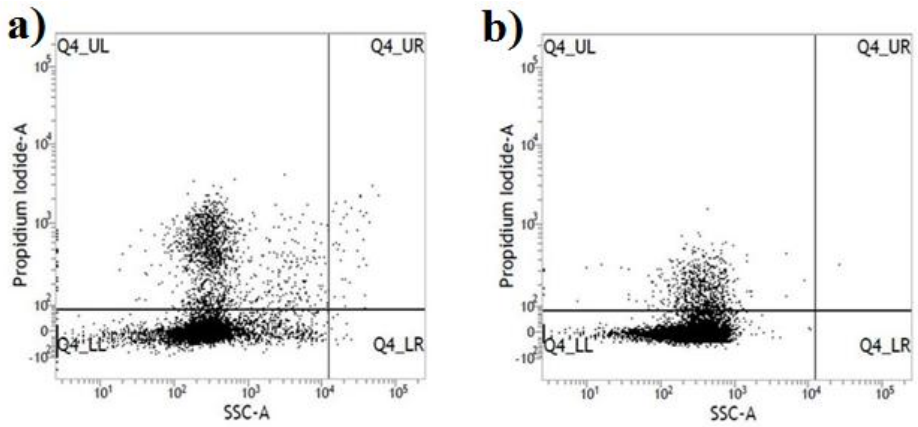

Figure 4.17 (a) lymphocytes treated with 10 mM of Nicotine only and (b) lymphocytes treated with 10 mM of nicotine +160 µg/ml of PS-II.

4.2.4.5. DPPH radicals scavenging ability

DPPH is a well-known radical which demonstrates a strong absorption peak at about 520 nm. It becomes pale yellow when neutralized. This radical is scavenged by antioxidants via donation of proton and is mostly used to evaluate the radical scavenging capacity of any antioxidants [251]. The scavenging activity of PS-II against the DPPH radical was shown in **Figure 4.18.** Results showed that both vitamin C and PS-II possess the potential to neutralize the DPPH radical and this activity was concentration-dependent at the ranges of 0.5–2.0 mg/ml. This study further validates the ROS scavenging ability of the PS-II which exhibited strong agreement with the previous experiments.

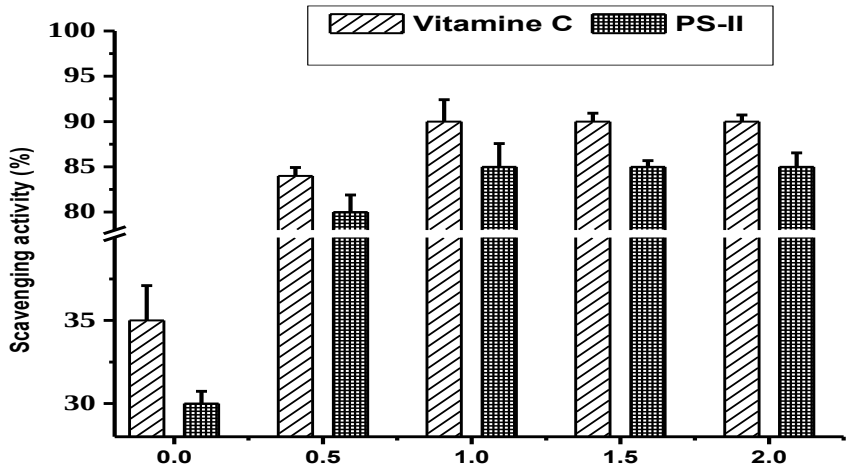

Figure 4.18. Scavenging ability of PS-II on DPPH radicals. (n = 4, values are expressed as mean±SEM. * Indicates the significant difference as compared to control group).

4.2.4.6. Nitric oxide assay for the test for macrophage activity

Activation of macrophage by PS-II was observed *in vitro* and noted that upon treatment with varied concentrations of PS-II, increase in the production of NO occured in a dose dependent manner with optimum production of 18 µM NO per 5 x 10^5 macrophages with an effective dosage of 80 µg/ml (**Figure 4.19**)..

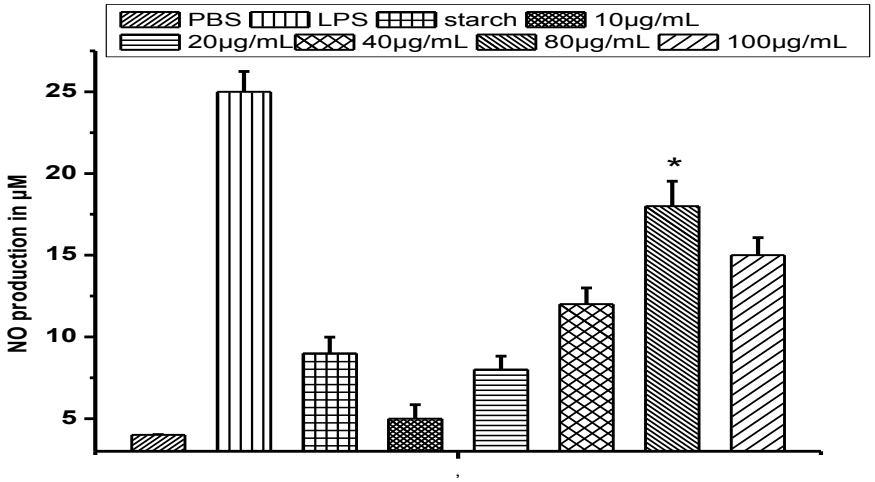

Figure 4.19. *In vitro* macrophage activation using different concentrations of PS-II (in terms of NO production). (n = 4, values are expressed as mean±SEM. * Indicates the significant difference as compared to control group).

4.2.4.7. Splenocyte proliferation assay

Proliferation of splenocytes is an indicator of immunoactivation. The splenocyte activation tests were carried out in mouse cell culture medium impregnated with the PS-II using SRB assay [243]. PS-II was tested to stimulate splenocytes and the results were shown in **Figure** 4.20. At 20 µg/ml of PS-II maximum splenocyte proliferation index (SPI) was obtained, above or below which it decreases. In a separate study it was noted that 25 µg/ml of LFPS extracted from *A. junii* BB1A exhibited maximum SPI [252].

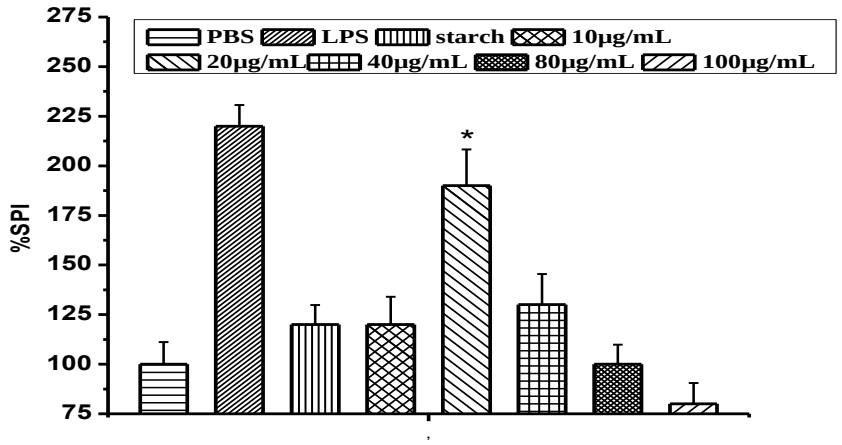

Figure 4.20. Effect of varied concentrations of PS-II on splenocyte proliferation. (n = 4, values are expressed as mean±SEM. * Indicates the significant difference as compared to control group).

4.2.5. Conclusion

A water soluble heteroglycan (PS-II), with an average molecular weight ~ 60 kDa, was isolated from the hot aqueous extract of an edible mushroom *L. fusipes* and the following structure was characterized by chemical analysis and 1D/2D NMR studies:

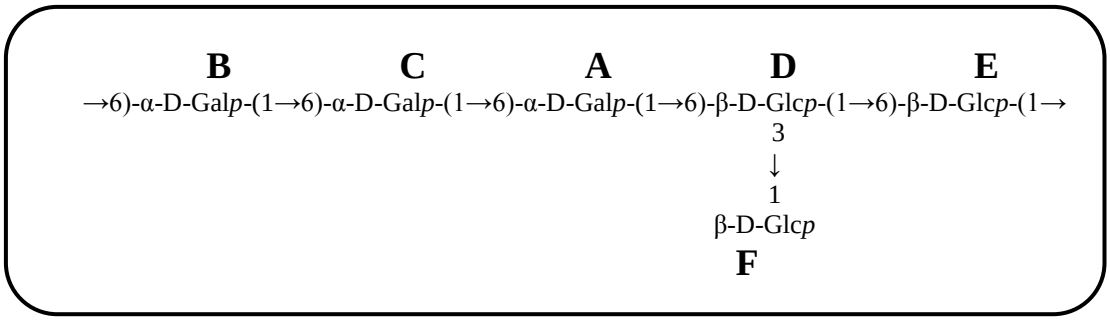

The polysaccharide showed no efficacy towards lipid peroxidation up to 160 µg/ml. PS-II does not exhibit any cellular toxicity and play a beneficial role on cell proliferation and its protection against nicotine stimulated toxicity. It was noted that the optimum concentration of PS-II for NO production and splenocyte proliferation was found to be 80 µg/ml and 20 µg/ml respectively.